

# Applicability of shape parameterizations for giant dipole resonance in warm and rapidly rotating nuclei

P. Arumugam <sup>a,1</sup>, A. Ganga Deb <sup>b</sup> and S. K. Patra <sup>a</sup>

<sup>a</sup>*Institute of Physics, Sachivalaya Marg, Bhubaneswar - 751 005, India.*

<sup>b</sup>*Sonepur College, Subarnapur - 767017, Orissa, India.*

---

## Abstract

We investigate how well the shape parameterizations are applicable for studying the giant dipole resonance (GDR) in nuclei, in the low temperature and/or high spin regime. The shape fluctuations due to thermal effects in the GDR observables are calculated using the actual free energies evaluated at fixed spin and temperature. The results obtained are compared with Landau theory calculations done by parameterizing the free energy. We exemplify that the Landau theory could be inadequate where shell effects are dominating. This discrepancy at low temperatures and high spins are well reflected in GDR observables and hence insists on exact calculations in such cases.

*Key words:* Giant dipole resonance, thermal fluctuations, Landau theory, hot rotating nuclei

---

In recent years considerable interest has been shown [1,2,3,4] to study the structural transitions as a function of both angular momentum and temperature in highly excited nuclei. The Giant Dipole Resonance (GDR) studies have been proved to be a powerful tool to study such hot and rotating nuclei [5] and recently the domain of GDR spreads rapidly over different areas of theoretical and experimental interest [6,7,8,9]. The GDR observations provide us information about the geometry as well as the dynamics of nuclei even at extreme limits of temperature ( $T$ ), spin ( $I$ ) and isospin ( $\tau$ ). In the past most of the GDR measurements in hot nuclei were made at moderate and high  $T$  [5,6,7,8,9,10,11,12]. Few experiments have been carried out recently to study the GDR states at low temperatures [1,2,3]. Hence the theories which were successful in the high  $T$  regime should be now scrutinized with the low

---

<sup>1</sup> *E-mail address:* aru@iopb.res.in

temperature observations as well as with theories incorporating properly the microscopic effects (such as shell effects) which are dominant at low temperatures. In a macroscopic approach, while dealing with the thermal shape fluctuations, free energy parameterizations such as Landau theory [13,14,15] are usually employed to do timesaving calculations. In this work we survey the applicability of Landau theory by demanding consistency with exact calculations done without any parameter fitting.

The theoretical approach we follow is of three fold with models for 1) shape calculations, 2) relating the shapes to GDR observables and 3) considering the shape fluctuations due to thermal effects. For shape calculations we follow the Nilsson-Strutinsky (NS) method extended to high spin and temperature [16]. The total free energy ( $F_{\text{TOT}}$ ) at fixed deformation is calculated using the expression

$$F_{\text{TOT}} = E_{\text{RLDM}} + \sum_{p,n} \delta F . \quad (1)$$

Expanding the rotating liquid-drop energy  $E_{\text{RLDM}}$  and writing shell corrections in rotating frame [17] leads to

$$F_{\text{TOT}} = E_{\text{LDM}} + \sum_{p,n} \delta F^\omega + \frac{1}{2} \omega (I_{\text{TOT}} + \sum_{p,n} \delta I) . \quad (2)$$

The angular velocity  $\omega$  is tuned to obtain the desired spin given by

$$I_{\text{TOT}} = \mathfrak{I}_{\text{rig}} \omega + \delta I . \quad (3)$$

The liquid-drop energy ( $E_{\text{LDM}}$ ) is calculated by summing up the Coulomb and surface energies [18] corresponding to a triaxially deformed shape defined by the deformation parameters  $\beta$  and  $\gamma$ . The rigid-body moment of inertia ( $\mathfrak{I}_{\text{rig}}$ ) is calculated with surface diffuseness correction [18]. The shell correction ( $\delta F^\omega$ ) is the difference between the deformation energies evaluated with a discrete single-particle spectrum and by smoothing (averaging) that spectrum and is given by the relation

$$\delta F^\omega = F^\omega - \tilde{F}^\omega = \left( \sum_{i=1}^{\infty} e_i^\omega n_i - T \sum_{i=1}^{\infty} s_i \right) - \left( \sum_i e_i^\omega \tilde{n}_i - T \sum_i \tilde{s}_i \right) , \quad (4)$$

where the discrete quantities

$$n_i = \frac{1}{1 + \exp\left(\frac{e_i^\omega - \lambda}{T}\right)} , \quad (5)$$

$s_i = -[n_i \ln n_i - (1 - n_i) \ln(1 - n_i)]$ , the Strutinsky smeared quantities  $\tilde{n}_i = \int_{-\infty}^{\infty} \tilde{f}(x) n_i(x) dx$ ,  $\tilde{s}_i = \int_{-\infty}^{\infty} \tilde{f}(x) s_i(x) dx$  and  $\tilde{f}(x)$  is the smearing function [16]. Similarly the shell correction corresponding to the spin is given by

$$\delta I = I - \tilde{I} = \sum_{i=1}^{\infty} m_i n_i - \sum_{i=1}^{\infty} m_i \tilde{n}_i . \quad (6)$$

The single-particle energies ( $e_i^\omega$ ) and spin projections ( $m_i$ ) are obtained by diagonalizing the triaxial Nilsson Hamiltonian in cylindrical representation upto first twelve major shells.

In a macroscopic approach, the GDR observables are related to the nuclear shapes. This is realized using a model [19] comprising an anisotropic harmonic oscillator potential with separable dipole-dipole interaction. In this formalism the GDR frequencies in laboratory frame are obtained as

$$\tilde{\omega}_z = (1 + \eta)^{1/2} \omega_z , \quad (7)$$

$$\begin{aligned} \tilde{\omega}_2 \mp \Omega = & \left\{ (1 + \eta) \frac{\omega_y^2 + \omega_x^2}{2} + \Omega^2 + \frac{1}{2} \left[ (1 + \eta)^2 (\omega_y^2 - \omega_x^2)^2 \right. \right. \\ & \left. \left. + 8\Omega^2 (1 + \eta) (\omega_y^2 + \omega_x^2) \right]^{\frac{1}{2}} \right\}^{\frac{1}{2}} \mp \Omega , \end{aligned} \quad (8)$$

$$\begin{aligned} \tilde{\omega}_3 \mp \Omega = & \left\{ (1 + \eta) \frac{\omega_y^2 + \omega_x^2}{2} + \Omega^2 - \frac{1}{2} \left[ (1 + \eta)^2 (\omega_y^2 - \omega_x^2)^2 \right. \right. \\ & \left. \left. + 8\Omega^2 (1 + \eta) (\omega_y^2 + \omega_x^2) \right]^{\frac{1}{2}} \right\}^{\frac{1}{2}} \mp \Omega , \end{aligned} \quad (9)$$

where  $\Omega$  is the cranking frequency,  $\omega_x$ ,  $\omega_y$ ,  $\omega_z$  are the oscillator frequencies derived from the deformation of the nucleus and  $\eta$  is a parameter that characterizes the isovector component of the neutron and proton average field. The GDR cross sections are constructed as a sum of Lorentzians given by

$$\sigma(E_\gamma) = \sum_i \frac{\sigma_{mi}}{1 + \left( E_\gamma^2 - E_{mi}^2 \right)^2 / E_\gamma^2 \Gamma_i^2} , \quad (10)$$

where Lorentz parameters  $E_m$ ,  $\sigma_m$  and  $\Gamma$  are the resonance energy, peak cross-section and full width at half maximum respectively. Here  $i$  represents the number of components of the GDR and is determined from the shape of the nucleus [19,20]. The energy dependence of the GDR width can be approximated by [21]

$$\Gamma_i \approx 0.026 E_i^{1.9} . \quad (11)$$

The peak cross section  $\sigma_m$  is given by

$$\sigma_m = 60 \frac{2}{\pi} \frac{NZ}{A} \frac{1}{\Gamma} 0.86(1 + \alpha) . \quad (12)$$

The parameter  $\alpha$  which takes care of the sum rule is fixed at 0.3 for all the nuclei considered in this work. In most of the cases we normalize the peak

with the experimental data and hence the choice of  $\alpha$  has less effect on the results. The other parameter  $\eta$  varies with nucleus so that the ground state GDR centroid energy is reproduced. The choice for  $^{84}\text{Zr}$  is  $\eta = 2.6$ , for  $^{147}\text{Eu}$ ,  $\eta = 2.8$ , for  $^{179}\text{Au}$ ,  $\eta = 3.2$ , and for  $^{208}\text{Pb}$ ,  $\eta = 3.4$ . For calculating the GDR width, only the power law (11) is used in this work and no ground state width is assumed.

When the nucleus is observed at finite excitation energy, the effective GDR cross-sections carry information on the relative time scales for shape rearrangements [22] which lead to shape fluctuations. In the case of hot and rotating nuclei, apart from thermal shape fluctuations, there can be fluctuations in the orientation of the nuclear symmetry axis with respect to the rotation axis. The general expression for the expectation value of an observable  $\mathcal{O}$  incorporating both thermal and orientation fluctuations is given by [13,23]

$$\langle \mathcal{O} \rangle_{\beta, \gamma, \Omega} = \frac{\int \mathcal{D}[\alpha] e^{-F(T, I; \beta, \gamma, \Omega)/T} (\hat{\omega} \cdot \mathcal{I} \cdot \hat{\omega})^{-3/2} \mathcal{O}}{\int \mathcal{D}[\alpha] e^{-F(T, I; \beta, \gamma, \Omega)/T} (\hat{\omega} \cdot \mathcal{I} \cdot \hat{\omega})^{-3/2}}, \quad (13)$$

where  $\Omega = (\phi, \theta, \psi)$  are the Euler angles specifying the intrinsic orientation of the system,  $\hat{\omega} \cdot \mathcal{I} \cdot \hat{\omega} = \mathfrak{I}_{x'x'} \cos^2 \phi \sin^2 \theta + \mathfrak{I}_{y'y'} \sin^2 \phi \sin^2 \theta + \mathfrak{I}_{z'z'} \cos^2 \theta$  is the moment of inertia about the rotation axis  $\hat{\omega}$  given in terms of the principal moments of inertia  $\mathfrak{I}_{x'x'}$ ,  $\mathfrak{I}_{y'y'}$ ,  $\mathfrak{I}_{z'z'}$ , and the volume element  $\mathcal{D}[\alpha] = \beta^4 |\sin 3\gamma| d\beta d\gamma \sin \theta d\theta d\phi$ .

The study of thermal fluctuations by numerical evaluation of Eq. (13) in general requires an exploration of five dimensional space spanned by the deformation and orientation degrees of freedom, in which a large number of points are required in order to assure sufficient accuracy (especially at finite angular momentum). Hence certain parameterizations were developed [14,24] to represent the free energy using functions that mimic the behaviour of the NS calculation as closely as possible. One such parametrization is the Landau theory of phase transitions, developed by Alhassid and collaborators [13,14,22,23]. Here the free energy is expanded in terms of certain temperature dependent constants which are to be extracted by fitting with the free energy calculations at fixed temperatures from the NS method. Moreover, once the fits involving free energy and moment of inertia are made for the non-rotating case, the calculations can be extended to higher spins using the relation [13]

$$F(T, I; \beta, \gamma, \Omega) = F(T, \omega = 0; \beta, \gamma) + \frac{(I + 1/2)^2}{2 \hat{\omega} \cdot \mathcal{I} \cdot \hat{\omega}}. \quad (14)$$

Hence this theory offers an economic parametrization to study the hot rotating nuclei. However the above expression carries the shell corrections evaluated at  $\omega = 0$  all along to higher spins. This is not desirable as the single-particle levels swiftly change positions with increasing spin, resulting in a totally different shell structure. We have employed Landau theory in its extended form as given

in Refs. [14,16].

Recently [16,25] few calculations have been done by performing the thermal fluctuation calculations exactly by computing the integrations in Eq. (13) numerically with the free energies and the observables being calculated “exactly” at the integration (mesh) points. In this way the calculations can be done more accurately without using any parametrization and consequent fitting. In this work we have performed such calculations, however, neglecting the orientation fluctuations. This enables us to perform the integration in the deformation space only which at present is two dimensional having the deformation parameters  $\beta$  and  $\gamma$ . The role of orientation fluctuations is negligible while calculating the scalar observables [16,26] such as the GDR cross section and width. The derivation [26] of Eq. 13 employs the assumption of Eq. (14) and here we discuss the consequences as the free energy now takes the form of Eq. (1). The partition function at fixed angular momentum  $I$  is obtained as [26]

$$Z_I(T) = \frac{2I+1}{2\pi iT^2} \int \mathcal{D}[\alpha] \left[ \int_{-i\infty}^{i\infty} d\omega \, \omega \, e^{-[\omega(I+1/2)+F\omega]/T} \right]. \quad (15)$$

The exponent in the above integral can be taken as  $-F_{\text{TOT}}/T$  in our case. Letting  $\hat{\omega} \cdot \mathcal{I} \cdot \hat{\omega} = \mathfrak{S}_{z'z'} = \mathfrak{S}_{\text{TOT}} = \mathfrak{S}_{\text{rig}} + \delta\mathfrak{S}$  and following the definitions given in Ref. [17], we have

$$d \left[ e^{-F_{\text{TOT}}/T} \right] = \mathfrak{S}_{\text{TOT}} \, \omega \, e^{-F_{\text{TOT}}/T} \, d\omega.$$

In the limit  $d\mathfrak{S}_{\text{TOT}}/d\omega \rightarrow 0$ , the integration over  $\omega$  in Eq. (15) is analytically solvable leading to an expression having exactly same form as Eq. (13) with  $\hat{\omega} \cdot \mathcal{I} \cdot \hat{\omega}$  replaced by  $\mathfrak{S}_{\text{TOT}}$ . The shell corrections to moment of inertia are significant for spherical shapes which are however suppressed by the term  $\beta^4$  in  $\mathcal{D}[\alpha]$  and for  $\beta \geq 0.1$  we have  $\mathfrak{S}_{\text{TOT}} \approx \mathfrak{S}_{\text{rig}}$ . At high spins also the limiting condition is very much valid as the well deformed shapes are more favoured. It has already been shown [26] that this transformation from frequency to angular momentum leads to a pre-factor to the volume element of the integral. However we show later that this factor has not much role to play in the practical calculations. While performing fluctuation calculations in this way, the free energy at any given spin is obtained by tuning the cranking frequency to get the desired spin. In such case the projection is not necessary and has been neglected in some similar calculations [25].

Now we compare our calculated results obtained by using the extended Landau theory and the exact method. The calculations are performed with 1) the liquid-drop model (LDM) free energies and Landau theory, 2) NS free energies and Landau theory and 3) NS free energies with exact treatment of fluctuations.

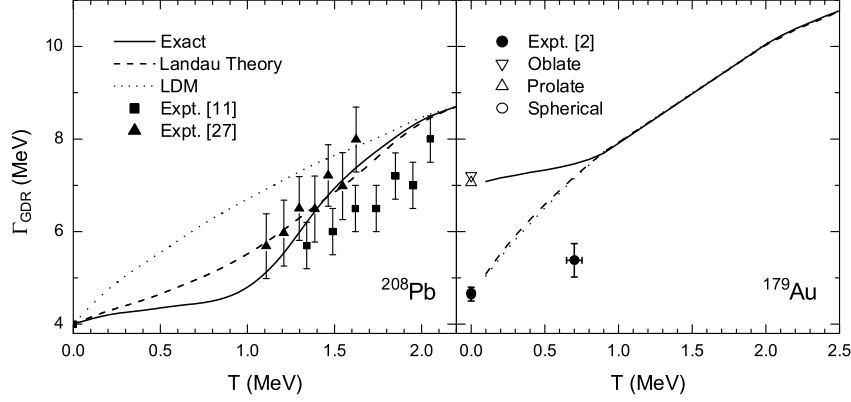


Fig. 1. GDR width for the nuclei  $^{208}\text{Pb}$  and  $^{179}\text{Au}$ . The results obtained using liquid drop model (dotted line), Landau theory (dashed line) and the exact calculations (solid line) are compared. *Left*: Experimental data represented by solid squares are taken from ref. [11] and the revised data [27] are represented by solid triangles. *Right*: The different curves carry same meaning as in the left panel. At  $T = 0$  MeV, the widths calculated assuming oblate ( $\beta_2 = -0.22$ ), prolate ( $\beta_2 = 0.24$ ) and spherical shapes are denoted by the open symbols down-triangle, up-triangle and circle respectively. The experimental value [2] at  $T = 0$  MeV is the intrinsic (spherical) width  $\Gamma_0$  and at  $T = 0.7$  MeV is the total width having  $\Gamma_0 = 5$  MeV and  $\beta_2 = 0.1$ . Both these values are represented by solid circles.

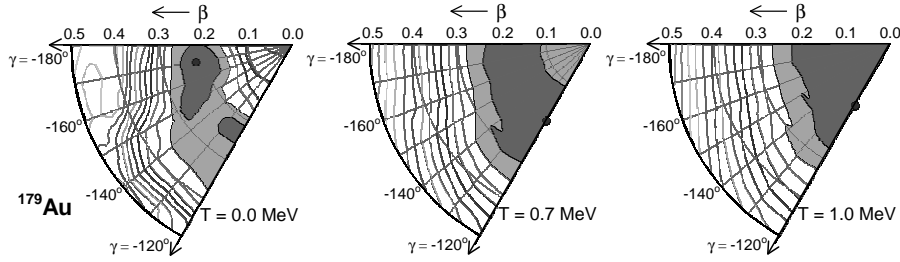


Fig. 2. Potential energy surfaces for  $^{179}\text{Au}$  at  $T = 0.0, 0.7$  and  $1.0$  MeV, calculated using the Nilsson-Strutinsky method. The contour line spacing in  $0.5$  MeV, the most probable shape is marked by a solid circle and the first two minima are shaded. The barrier between the co-existing shapes diminish with increase in temperature and the nucleus becomes  $\gamma$ -soft at  $T \sim 0.7$  MeV.

In Fig. 1 we present the calculated GDR widths of  $^{208}\text{Pb}$  and  $^{179}\text{Au}$  at  $\omega = 0$  along with experimental results. In the case of  $^{208}\text{Pb}$ , strong shell corrections for spherical shape results in large difference in the deformation energies between spherical and deformed configurations. This leads to attenuation of thermal fluctuations at lower temperature and hence the obtained widths are much lower when compared to liquid-drop model results. The magnitude of this attenuation comes out to be different in methods 2 and 3. More discussions and comparison with other reported results can be found in Ref. [16]. Recently [2] the thermal fluctuation calculations of  $^{208}\text{Pb}$  were extrapolated to interpret low  $T$  measurement of  $\Gamma_{GDR}$  in  $^{179}\text{Au}$ . This extrapolation was assumed to give the lower limit for the  $\Gamma_{GDR}$ . Our calculations as shown in Fig.

I do not favour any such interpretation. In fact the situation in  $^{179}\text{Au}$  is totally different from that of  $^{208}\text{Pb}$  as now deformed shapes are more favoured. The ground state deformation comes out in our calculations as  $\beta_2 = -0.22$  which is slightly larger than  $\beta_2 = -0.17$  obtained by relativistic mean field theory (with NL3 parameter set) and Hartree-Fock-Bogoliubov calculations [28].  $\Gamma_{GDR}$  calculated for this deformation at  $T = 0$  MeV lie very close to those obtained with exact thermal fluctuations at  $T = 0.1$  MeV. Moreover coexisting oblate and prolate shapes also prevail as we observe in the potential energy surfaces (PES) given in Fig. 2. We infer from the PES that the deformed shapes only are favoured even at  $T = 0.7$  MeV where we see  $\gamma$ -softness. As the  $\Gamma_{GDR}$  of deformed shapes are always higher than spherical ones, the calculation without shell effects (LDM), which favour spherical shapes, give the lower limit for  $\Gamma_{GDR}$  in deformed nuclei. Hence the inclusion of shell corrections will only increase  $\Gamma_{GDR}$  and could not account for the suppression of  $\Gamma_{GDR}$  in  $^{179}\text{Au}$ .

A similar situation has been observed in  $^{120}\text{Sn}$  [1] also where the thermal fluctuation model, even with shell effects included, could not explain the suppression of  $\Gamma_{GDR}$  at low  $T$ . Our exact calculations (see Fig. 4 of Ref. [16]) also could not explain this anomaly. It has been speculated [29] that this suppression could be a general feature of all nuclei, independent of shell effects. The possible cause of this could be the pairing correlations which can be significant at low  $T$ . The inclusion of fluctuations in the pairing field [30] or fully microscopic calculations [31] considering the temperature dependence of spreading width could explain the low width of  $^{120}\text{Sn}$  at low  $T$ . The same could be the case of  $^{179}\text{Au}$  also. In the present work, we wish to emphasis on the problems in using the shape parameterizations apart from these effects.

Also we infer from the calculations of  $^{208}\text{Pb}$  and  $^{179}\text{Au}$ , if the shell effects are strong leading to a crisp or multiple minima, the Landau theory could not account for it. This discrepancy can be partially ascribed to the parameterization itself and the fitting procedure involved. It was already suggested [14] that at low temperatures the least square fit for Landau constants could be erroneous and techniques like uniform mapping should be adopted. The new parameterization [24] may solve some of these issues despite having some inconsistencies at higher temperatures. However in both the methods involving shape parameterization, the high spin calculations are done using Eq. (14). Due to the complexity of shell structure at high spins, the difference in shell effects with changing spin may be crucial especially at lower temperatures.

In our previous work [16] we investigated the spin dependence of  $\Gamma_{GDR}$  in  $^{120}\text{Sn}$  at  $T = 1.8$  MeV (See Fig. 5 of Ref. [16]) and found the Landau theory to perform well even at spins upto  $70\hbar$ . This is understandable as there is no spin dependence of shell effects in this case and the temperature is sufficiently high where the Landau theory works well. Our results for  $^{179}\text{Au}$  at  $T = 0.7$  MeV and at different spins are shown in Fig. 3. Here also the spin dependence

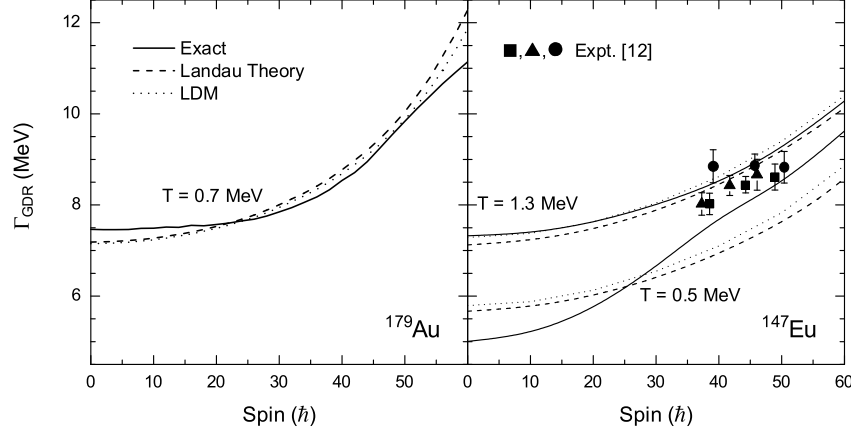


Fig. 3. Spin dependance of GDR width in  $^{179}\text{Au}$  and  $^{147}\text{Eu}$ . The results obtained using liquid drop model (dash-dotted line), Landau theory (dashed line) and the exact calculations (solid line) are compared. *Right:* The solid circle, solid square and solid triangle correspond to experimental data [12] at beam energies 170, 165 and 160 MeV respectively. These energies correspond to temperatures from 1.2 to 1.4 MeV [12].

of shell effects are found to be insignificant. We extended our study to  $^{147}\text{Eu}$  for which experimental data is available for  $T \sim 1.3$  MeV. Our results are shown in Fig. 3 where we can see that at  $T = 1.3$  MeV there is not much difference between the results of Landau theory and exact calculations. Also the widths are very much similar to those obtained using LDM as the proton and neutron shell corrections are weak and they act against themselves. This trend continues even at spins up to  $60\hbar$ . However at  $T = 0.5$  MeV, the situation is drastically different as the spin-driven shell effects play their role. At  $\omega = 0$ , the shell correction is of the order of 2 MeV and hence the three methods give different results. The shell corrections decrease with the increasing spin, at  $40\hbar$  the equilibrium shape acquires deformation  $(\beta, \gamma) = (0.3, -180^\circ)$  and at  $60\hbar$ , it is  $(0.3, -130^\circ)$ . The effect of these sharp changes survive thermal fluctuations in the exact calculations and is averaged out in the Landau theory as well as the LDM calculations. It has to be noted that the Landau theory results carry the shell corrections calculated at  $\omega = 0$  all along. From the above arguments it is clear that one cannot substantiate the success of Landau theory in the cases of  $^{120}\text{Sn}$  and  $^{179}\text{Au}$ . For certain nuclei like  $^{147}\text{Eu}$  the spin-driven shell effects can be crucial at low  $T$ .

In Fig. 4 we show for the hot rotating  $^{84}\text{Zr}$  nucleus, the results of our GDR cross section calculations. It has been observed that in neutron-deficient Zr isotopes, spin-driven shell effects are stronger leading to a sharp shape transition at lower temperatures [16]. It is evident from the Fig. 4 that, in certain nuclei at higher spins the spin-driven shell effects may play vital role even at  $T \sim 1$  MeV. Also we show in Fig. 2 the impact of including the pre-factor  $\mathfrak{S}_{\text{TOT}}^{-3/2}$  in the thermal fluctuation integral. This is the only case presented in this work where we could notice a slight effect of the factor. One can observe that



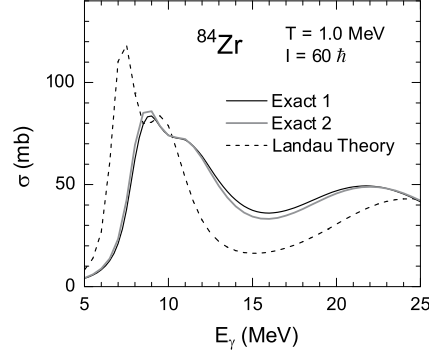


Fig. 4. GDR cross sections for the nuclei  $^{84}\text{Zr}$  at  $T = 1.0$  MeV and  $I = 60\hbar$  with shape fluctuations using Landau theory (dashed line), exact method with the factor  $\mathfrak{S}_{\text{TOT}}^{-3/2}$  (Exact 1, solid black line) and exact method without that factor (Exact 2, solid grey line).

even at extreme limits of spin the pre-factor has practically no effect as the dominating role is played by the exponential term  $\exp(-F_{\text{TOT}}/T)$  which has exact temperature and spin dependence.

To summarize, in this work the thermal fluctuations are dealt in an exact way without any parameter fitting. Comparison of our present approach with the thermal fluctuation model comprising Landau theory suggests that the shape parameterizations could be insufficient for GDR calculations in the presence of strong shell effects. The discrepancies are shown in certain nuclei at two situations namely at very low temperatures ( $T < 1$  MeV) and at moderate temperatures and high spin ( $T \sim 1$  MeV,  $I \gtrsim 30\hbar$ ). The latter case is ascribed to spin driven shell effects, which the existing shape parametrizations do not account for. The present study necessitates exact treatment of fluctuations in these cases where there is experimental and theoretical focus recently.

## References

- [1] P. Heckman, et al., Phys. Lett. B **555** (2003) 43.
- [2] F. Camera, et al., Phys. Lett. B **560** (2003) 155.
- [3] A. Bracco, Acta Phys. Pol. B **34** (2003) 2163.
- [4] D. Kusnezov, and W.E. Ormand, Phys. Rev. Lett. **90** (2003) 042501.
- [5] K.A. Snover, Annu. Rev. Nucl. Part. Sci. **36** (1986) 545; J.J. Gaardhøje, Annu. Rev. Nucl. Part. Sci. **42** (1992) 483.
- [6] A. Maj, et al., Acta Phys. Pol. B **26** (1995) 417.
- [7] F. Camera, et al., Acta Phys. Pol. B **32** (2001) 807.

- [8] N. Tsoneva, Ch. Stoyanov, Yu.P. Gangrsky, V.Yu. Ponomarev, N.P. Balabanov, and A.P. Tonchev, Phys. Rev. C **61** (2000) 044303.
- [9] I. Diószegi, I. Mazumdar, N.P. Shaw, and P. Paul, Phys. Rev. C **63** (2001) 047601.
- [10] J. Gundlach, K.A. Snover, J.A. Behr, C.A. Gossett, M.K. Habior, and K.T. Lesko, Phys. Rev. Lett. **65** (1990) 2523.
- [11] T. Baumann, et al., Nucl. Phys. A **635** (1998) 428.
- [12] M. Kmiecik, et al., Nucl. Phys. A **674** (2000) 29.
- [13] Y. Alhassid, Nucl. Phys. A **649** (1999) 107c.
- [14] Y. Alhassid and B. Bush, Nucl. Phys. A **549** (1992) 12.
- [15] G. Shanmugam and V. Selvam, Phys. Rev. C **62** (2000) 014302.
- [16] P. Arumugam, G. Shanmugam and S.K. Patra, Phys. Rev. C **69** (2004) 054313.
- [17] K. Neergård, V.V. Pashkevich and S. Frauendorf, Nucl. Phys. **A262**, (1976) 61.
- [18] G. Shanmugam, V. Ramasubramanian and P. Arumugam, Pramana - J. Phys. **53** (1999) 457; G. Shanmugam, V. Ramasubramanian and S.N. Chintalapudi, Phys. Rev. C **63** (2001) 064311.
- [19] G. Shanmugam and M. Thiagasundaram, Phys. Rev. C **37** (1988) 853; Phys. Rev. C **39** (1989) 1623.
- [20] R.R. Hilton, Z. Phys. A **309** (1983) 233.
- [21] P. Carlos, R. Bergere, H. Beil, A. Lepretre and A. Veyssiere, Nucl. Phys. A **219** (1974) 61.
- [22] Y. Alhassid and B. Bush, Nucl. Phys. A **509** (1990) 461.
- [23] Y. Alhassid and B. Bush, Nucl. Phys. A **531** (1991) 39.
- [24] W.E. Ormand, P.G. Bortignon, R.A. Broglia and A. Bracco, Nucl. Phys. A **614** (1997) 217.
- [25] A. Ansari, N.D. Dang and A. Arima, Phys. Rev. C **63** (2003) 024310.
- [26] W.E. Ormand, P.G. Bortignon and R.A. Broglia, Nucl. Phys. A **618** (1997) 20.
- [27] D. Kusnezov, Y. Alhassid and K.A. Snover, Phys. Rev. Lett. **81** (1998) 542.
- [28] M. Samyn, S. Goriely, P.-H. Heenen, J. M. Pearson and F. Tondeur, Nucl. Phys. **A700** (2001) 142.
- [29] M. Thoennessen, Nucl. Phys. A **731** (2004) 131.
- [30] N.D. Dang and A. Arima, Phys. Rev. C **68** (2003) 044303.
- [31] A.N. Storozhenko, A.I. Vdovin, A. Ventura and A.I. Blokhin, Phys. Rev. C **69** (2004) 064320.